Hindawi
Advances in Civil Engineering
Volume 2023, Article ID 4596750, 10 pages
https://doi.org/10.1155/2023/4596750

Research Article

Effect of Temperature on Interface Characteristics between Compacted Recycled Asphalt Pavement and Geogrid

Lin Liu,[1] Zhaoer Zhang,[1] Lexuan Zhang,[1] Yong Tang,[2] and Jie Yin [1]

[1]*Department of Civil Engineering, Faculty of Civil Engineering and Mechanics, Jiangsu University, Zhenjiang 212013, China*
[2]*Jiangsu Sutong Bridge Co. Ltd., Nantong 226000, China*

Correspondence should be addressed to Jie Yin; yinjie@ujs.edu.cn

Received 3 April 2023; Revised 2 August 2023; Accepted 25 August 2023; Published 9 September 2023

Academic Editor: Xia Bian

This study presents an experimental investigation of the interface behaviors of recycled asphalt pavement (RAP) reinforced with biaxial geogrid. A series of direct shear tests were conducted on compacted RAP specimens with or without geogrid under different normal stresses (50, 75, and 100 kPa) and test temperatures (0, 20, and 35°C) using an improved temperature-controlled direct shear apparatus. The effect of test temperature on interface shear strength and strength parameters was systematically examined. Test results showed that shear stress versus shear displacement curves of RAP specimens with or without geogrid show strain-softening characteristics. Under the same normal stress, the curve of the reinforced RAP sample with a high temperature is always below that with a low temperature, which indicates the test temperature has an adverse effect on the strength of the reinforced RAP sample. The shear strength consistently increases linearly with the increase of applied normal stress for all RAP samples. The shear strength with geogrid is greater than pure RAP under a given test temperature and normal stress. The shear strength of RAP samples at lower test temperatures is higher than that at a higher temperature. Both apparent adhesion intercept of RAP-geogrid and cohesion of RAP show a decreasing trend with the increase of the test temperature and tend to be stable with increasing temperature. Both the interface friction angle of RAP-geogrid and the internal friction angle of RAP slightly decrease with the increase of test temperature. For RAP-geogrid, the value of the apparent adhesion intercept is higher than that for sand and gravel with geosynthetics. The interface friction angle is close to that of sand and gravel with geosynthetics. Therefore, RAP material can be well used as alternative backfill materials in lieu of natural aggregates such as gravel and sand in geotechnical applications.

1. Introduction

Recycled materials are increasingly used as an alternative source of aggregates to promote sustainable construction practices. The beneficial use of recycled materials not only reduces the consumption of energy and natural resources but also decreases emissions of greenhouse gases associated with mining, production, and transport of conventional construction aggregates [1–4]. Recycled asphalt pavement (RAP) is produced by removing and reprocessing existing asphalt pavements. Approximately 790 million tons of RAP are produced annually in China [5]. The frequency of beneficial use of RAP in China, however, is only about 30%, which is much lower than 80% in the United States and other countries [5], indicating that the beneficial use of RAP has great potential. RAP is most commonly used as a substitute for virgin aggregate or virgin asphalt binder in asphalt paving [6, 7] but may also be used as granular base or subbase material, stabilized base aggregate, and embankment or structural backfill material in geotechnical applications [8–14].

Unlike conventional materials, the asphalt binder coating on RAP particles increases the material's compressibility and may lead to excessive long-term deformations under sustained deviator stresses present in embankments and retained fills [15, 16]. Creep for soils and aggregates is the accumulation of time-dependent shear strain under sustained shear stress that is controlled by the viscosity of the material structure [17–20]. Since the viscosity of asphalt binder is temperature-sensitive [21], temperature changes expected in field applications may also affect the creep characteristics and performance of RAP as an alternative construction material. Soleimanbeigi et al. [16] reported results from laboratory tests showing that higher temperatures increased the compressibility of RAP. Yin et al. [3] investigated the effects of elevated temperatures on the creep behavior of compacted RAP specimens through temperature-controlled triaxial compression tests at sustained deviator stresses and characterized the creep of compacted RAP at elevated temperatures. Therefore, the influence of temperature on RAP material cannot be ignored. Besides, an effective way to alleviate the creep deformation of RAP is to add geosynthetics such as geomembrane, geotextile, and geogrid [22, 23]. Thakur et al. [22] found that the restriction of geogrid can increase the rigidity of RAP material and also reduce its creep deformation. Soleimanbeigi et al. [23] evaluated the mechanical and hydraulic properties of RAP as backfill reinforced with woven and nonwoven geotextiles and uniaxial and biaxial geogrids in mechanically stabilized earth walls. Results of interface direct shear tests showed that the interface friction angle is the biggest for RAP-biaxial geogrid [23].

It should be noted that the previous research suggested that increasing compaction temperature notably increases the shear strength of compacted RAP [3, 16]. For unreinforced compacted RAP, increasing compaction temperature densifies the specimen and increases the particle contact surfaces, thus increasing the shear strength [16]. Moreover, for geosynthetics-reinforced compacted RAP, densifying RAP specimens at elevated compaction temperatures may not necessarily increase the interface friction between RAP particles and geosynthetics [23]. Noted that existing studies mainly focused on the impact of compaction temperature. The effect of temperature during the testing period, however, has not been well understood, especially for interface characteristics between compacted RAP and geosynthetics. This study aims at investigating the effect of experimental temperature on the interface shear behavior of RAP-geosynthetics. A series of direct shear tests were carried out on RAP-geosynthetics under different experimental temperatures to study the interface strength and friction parameters of reinforced RAP. The interfacial shear tests of reinforced RAP samples under different normal stresses were conducted at various experimental temperatures using the improved temperature-controlled strain type direct shear instrument, and the results were compared with those of pure RAP samples. The influence of test temperature on interface shear strength and friction characteristics of RAP-geogrid were evaluated.

2. Materials and Methods

2.1. Materials

2.1.1. RAP. A representative bulk sample of granular RAP was obtained from a local road maintenance company in Zhenjiang, China. The asphalt binder content of the material obtained per ASTM [24] was 4.2% by weight, which is within the typical 3%–7% for RAP [10, 25]. Visual observation indicated that the majority of the RAP particles were coated with asphalt binder (Figure 1). The grain-size distribution retain of the RAP (Figure 2) obtained per ASTM [24] retain indicated that the RAP sample was classified as well-graded sand (SW) according to the unified soil classification system

FIGURE 1: Photograph of RAP particles.

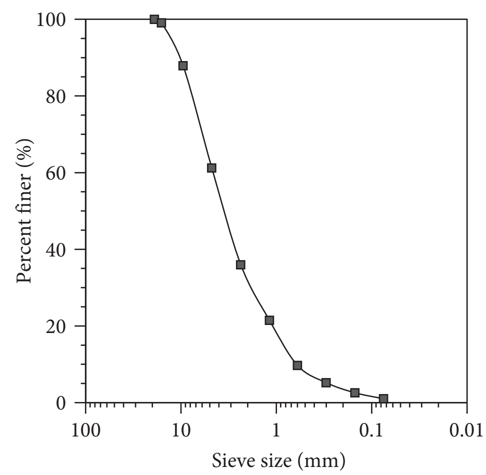

FIGURE 2: Grain size distribution curve.

(USCS). Based on the grain size distribution curve, the coefficient of curvature ($C_c = 1.28$), coefficient of uniformity ($C_u = 7.84$), and the effective sizes ($d_{10} = 0.61$ mm, $d_{30} = 1.93$, and $d_{60} = 4.78$) can be obtained, and it is classified as well graded RAP. The specific gravity (G_s) of the RAP solids (from ASTM [26], retain Method B) was 2.42, which is within the typical range of 2.2–2.56 for RAP [25]. The specific gravity of RAP is lower than that of natural aggregates (2.65–2.70) and is attributed to the material's asphalt binder coating. Figure 3 shows the compaction curve of the RAP sample obtained using standard Proctor effort per ASTM [27], retain indicating the optimum water content (w_{opt}) of 5.1% and maximum dry density (ρ_{dmax}) of 1.88 g/cm^3. These values are also within the range of values reported for different sources of RAP [25].

2.1.2. Geogrids. The geogrid used in this paper was polypropylene biaxial geogrid, with a net mesh size of 20 mm × 20 mm, rib width of 2.2 mm, thickness of 0.09 mm, and joint thickness of 2.2 mm. Its mechanical performance indexes are shown in Table 1. The reason of selecting the biaxial geogrid is because the biaxial geogrid exhibited a higher interface friction angle than that of the uniaxial geogrid [23].

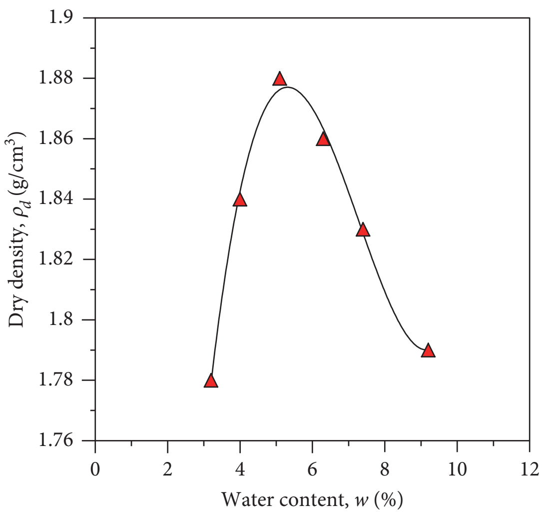

Figure 3: Standard proctor compaction curve of RAP.

Table 1: Biaxial geogrid physical parameters.

Tensile strength (kN/m)	Elongation rate (%)	Tensile force at 2% (kN/m)	Tensile force at 5% strain (kN/m)
11.76	8.58	5.01	9.14

2.2. Methods

2.2.1. Specimen Preparation. Before the test, the RAP sample was prepared at $w_{opt} = 5.1\%$ and put into a closed container, and stored in an oven at 50°C for 12 hr. A thermometer was embedded in the RAP sample to ensure that its temperature reached the preset compaction temperature of 50°C. The selection of 50°C is due to the fact that previous studies have shown that increasing compaction temperature will densify the specimen and increase the particle contact surfaces, thus increasing the shear strength [16]. Other studies also show similar results of RAP samples with the maximum strength at the compaction temperature of 50°C [23, 28]. For the case without geogrid, weigh a certain mass of RAP from the oven and directly place it into a direct shear box (upper and lower box in Figure 4) for compaction with four layers. The inner square size of the upper or lower box is designed as 100 mm × 100 mm and the height is 25 mm. Each specimen was compacted to obtain the target w_{opt} and 95% ρ_{dmax} in the shear box to achieve an identical initial state. Compaction was performed in four layers by a manual hammer to achieve the target density. For the case with geogrid, compaction was first conducted in two layers to fill the lower shear box; then, the geogrid was fixed between the upper and lower shear boxes. The compaction was continued with two layers to fill the upper box.

2.2.2. Direct Shear Tests (DSTs). DSTs were conducted on RAP samples compacted at room temperature in the modified shear box (with a square inner size of 100 mm × 100 mm) by conventional strain-controlled direct shear apparatus, as shown in Figure 4. The height is 25 mm for both upper and lower shear boxes. Table 2 shows the details of the testing program for compacted RAP specimens at 50°C with or without geogrid and direct sheared at different experimental temperatures (i.e., $T = 0$, 20, and 35°C) and normal stresses (i.e., $\sigma = 50$, 75, and 100 kPa). The reason of selecting different experimental temperatures is to reflect the representative temperature at different seasons. After compaction of the RAP sample with or without geogrid, the normal stress (i.e., $\sigma = 50$, 75, and 100 kPa) was applied to each specimen. The vertical compression of each specimen was recorded after each normal stress was applied. The direct test was thereafter run at a shearing rate of 1 mm/min [29] retain. The horizontal displacements were recorded by a linear variable differential transformer placed outside of the upper half of the shear box.

To realize the test temperature (i.e., $T = 0$, 35°C) other than room temperature (20°C), a self-made thermal insulation device was used with a main iron box with thermal insulation cotton (Figure 5(a)) and wrapped with the polyimide electric thermal film arranged on the four inner walls of the iron box to realize the heating function (Figure 5(a)) or mounted the XD-148 type refrigerator (Figure 5(b)) on the top of the iron box to realize the cooling function. The XH-W2403 type digital time and temperature controller (Figure 5(c)) was connected to automatically control the on–off of the heating and cooling device to maintain the direct shear test temperature within ±1°C.

3. Results and Discussion

Figure 6 shows the relationship curves between shear stress and shear displacement of reinforced and unreinforced RAP samples under different normal stress obtained through direct shear tests, where Figures 6(a), 6(b), and 6(c), respectively, represent the test results under different conditions at 0, 20, and 35°C. On the whole, unreinforced RAP and reinforced RAP samples are similar to traditional coarse-grained soils, showing a consistent trend with significant peak shear stress and strain-softening characteristics. The peak shear stress τ_f of each curve represents the shear strength of the corresponding sample under the vertical load. After the peak strength, the shear stress decreases gradually, which may be caused by the slip between the geogrid ribs and RAP particles at the shear boundary. It can be seen that the peak stress of the reinforced RAP samples is higher than that of the unreinforced RAP samples under the same working conditions. Taking Figure 6(a) as an example, when the normal stress $\sigma = 50$, 75, and 100 kPa, the corresponding peak shear stresses of the reinforced RAP sample are 94.3, 117.3, and 140.6 kPa, respectively. The corresponding peak shear stresses of unreinforced RAP samples are 88.6, 115.2, and 135.6 kPa, respectively. These results indicate that the peak shear stress of the reinforced RAP sample is improved compared with the pure RAP sample. The possible reason is that the interaction between geogrid and RAP particles in reinforced RAP samples is composed of friction resistance and interlock resistance [23, 30]. The friction resistance is mainly provided by the friction between the geogrid rib surfaces and

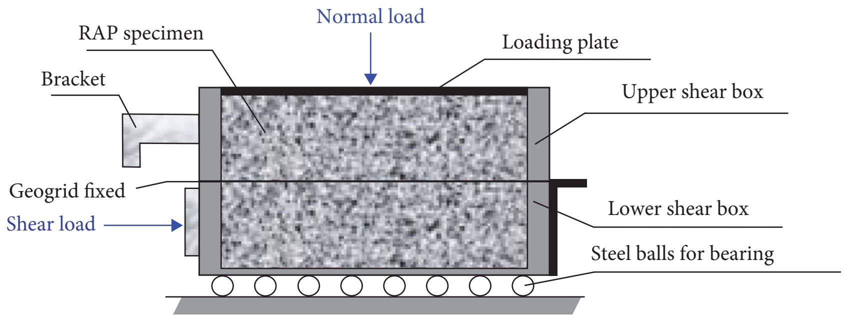

FIGURE 4: Schematic diagram of direct shear apparatus.

TABLE 2: Direct shear testing program.

Items	Compaction temperature T (°C)	Test temperature T (°C)	Normal stress σ (kPa)
RAP with geogrid	50	0, 20, 35	50, 75, 100
Unreinforced RAP	50	0, 20, 35	50, 75, 100

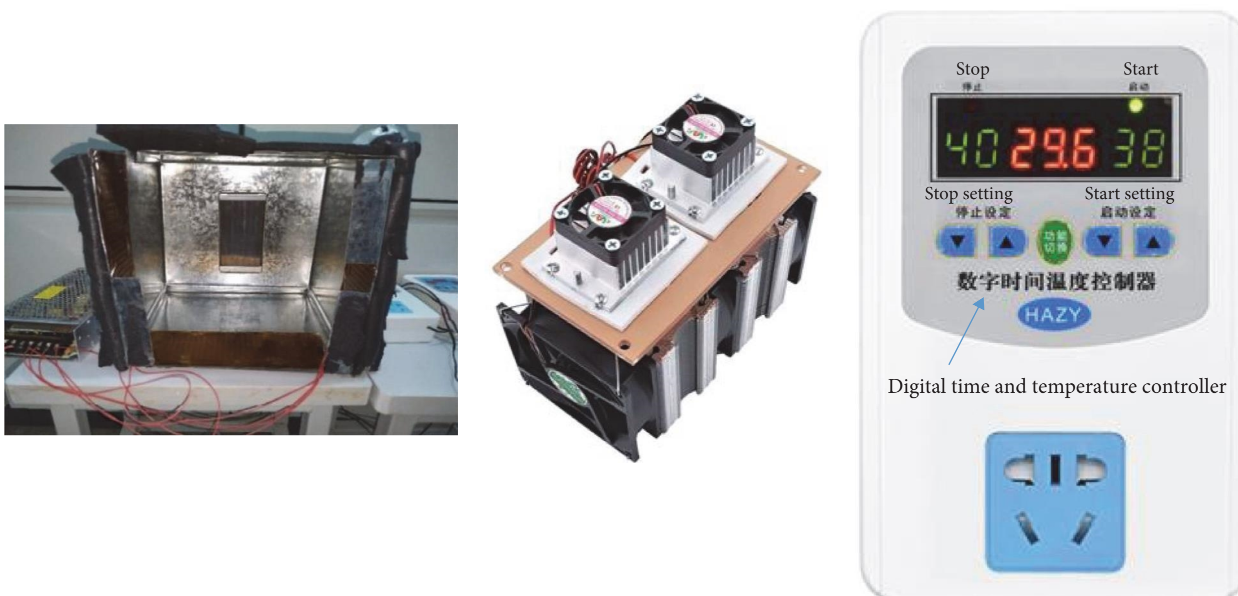

(a) (b) (c)

FIGURE 5: Photographs of thermal insulation device (a) iron box with thermal insulation cotton and polyimide electric thermal film, (b) XD-148 refrigerator, and (c) XH-W2403 temperature controller.

RAP particles. The geogrid openings also provide significant passive resistance at the interface between the geogrid ribs and RAP. The interlock resistance is mainly generated across the geogrid rib surfaces between RAP particles.

To evaluate the influence of test temperature on the interface characteristics of reinforced RAP backfills, Figure 7 shows the variation of shear stress with shear displacement for reinforced RAP samples at a given normal stress at three different test temperatures (0, 20, and 35°C). It can be seen that under the same normal stress, the curve of the reinforced RAP sample with a high temperature is always below that with a low temperature. For example, as the normal stress $\sigma = 75$ kPa, the peak stresses of geogrid-reinforced RAP samples were 117.3 kPa at 0°C, 100.4 kPa at 20°C, and 94.6 kPa at 35°C, respectively. It indicates that the test temperature has an adverse effect on the strength of the reinforced RAP sample, and the higher the test temperature, the lower the strength of the reinforced RAP sample. The main reason is that RAP material with asphalt binder is sensitive to the change in temperature. With the increase in temperature, asphalt will suffer heat softening, and its viscosity gradually increases, which in turn reduces the bond strength between the geogrid and RAP material as well as between RAP particles decreases. Similar results have also been reported by other researchers; for example, Sudarsanan et al. [31] evaluated the influence of test

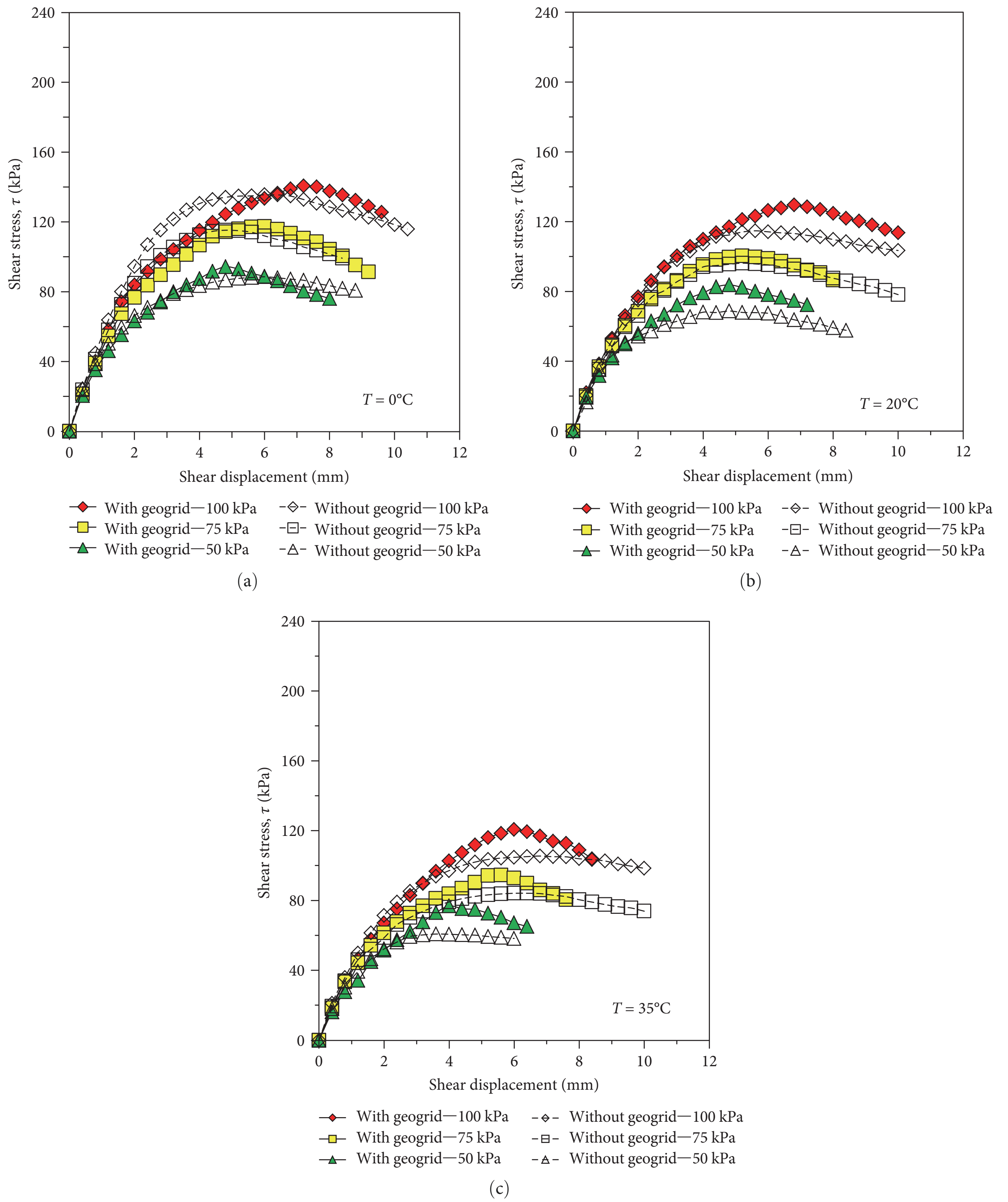

Figure 6: Variation of shear stress with shear displacement for non-reinforced and reinforced RAP specimens at (a) $T = 0°C$, (b) $T = 20°C$, and (c) $T = 35°C$ with different normal stresses.

temperature on the bond strength of the asphalt layer through experiments and found that when the temperature increased from 10 to 30°C, the bond strength of asphalt layer was significantly reduced by nearly 80%.

To further investigate the effect of test temperature on shear strength τ_f of RAP samples, Figure 8 shows the variation of shear strength with normal stress obtained from the direct shear test on RAP samples at different test temperatures. It

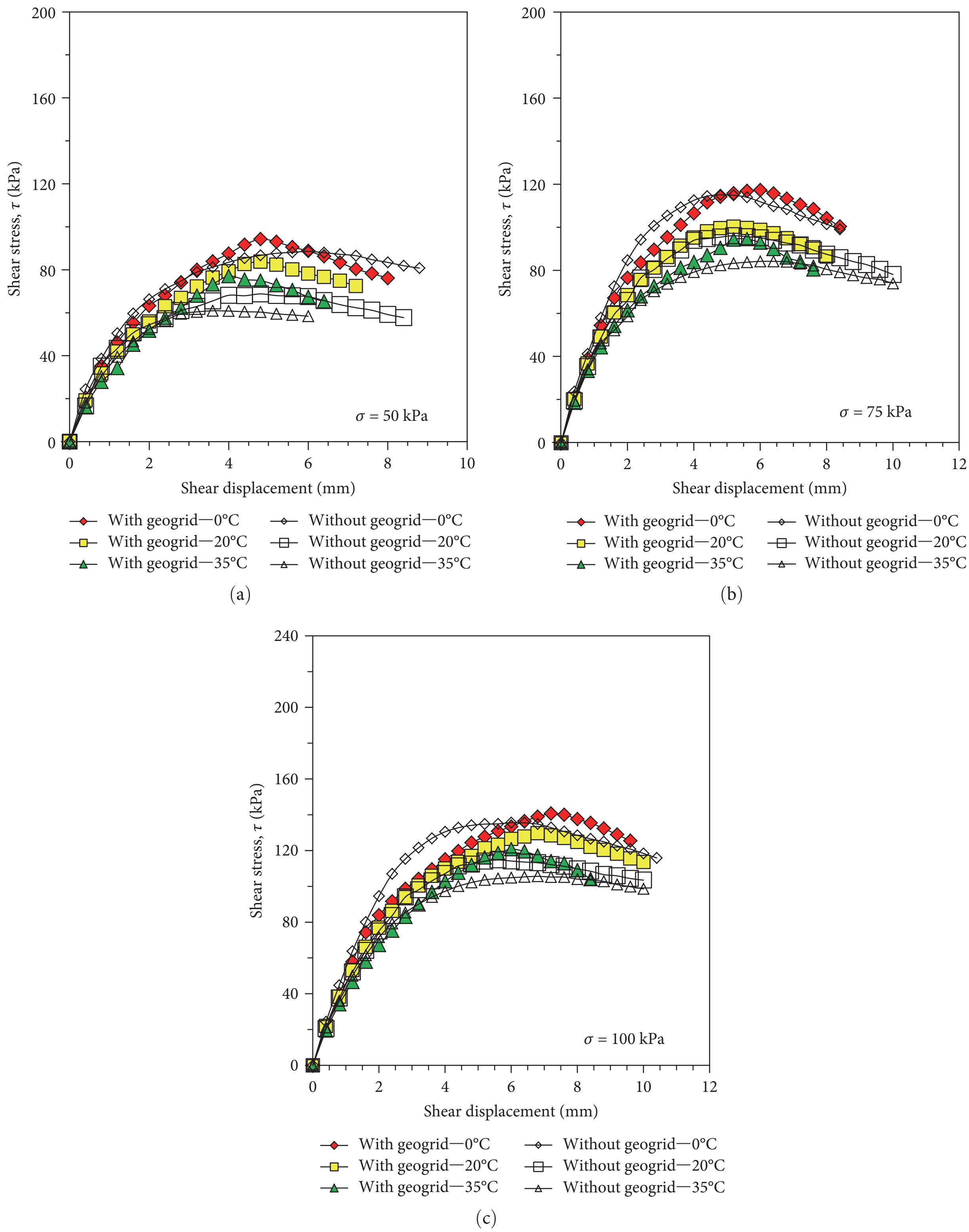

FIGURE 7: Variation of shear stress with shear displacement for reinforced RAP specimens at (a) 50 kPa, (b) 75 kPa, and (c) 100 kPa under different test temperatures.

can be seen that the shear strength τ_f consistently increases linearly with the increase of applied normal stress for all RAP samples with or without geogrid at different test temperatures. For comparison, test data from another study [23] were collected and plotted in Figure 8. They conducted the large-scale direct shear test for RAP with biaxial geogrid, woven, and unwoven geotextiles at 22°C. A similar ascending trend in shear strength with increasing applied normal stress

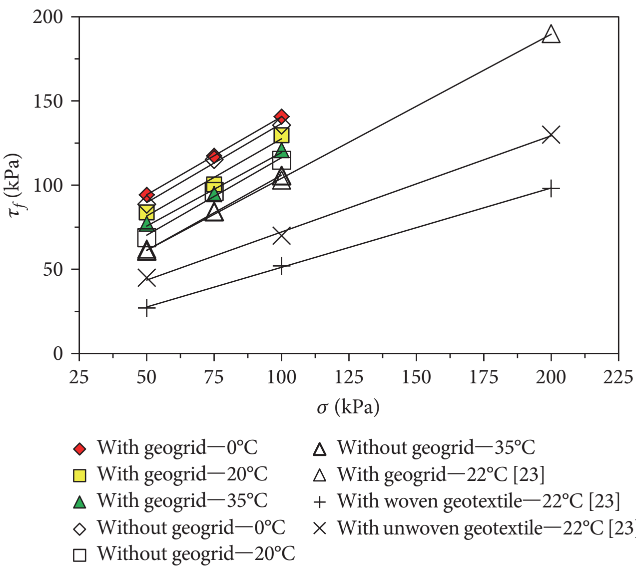

Figure 8: Variation of shear strength τ_f with normal stress σ for reinforced RAP specimens at different test temperatures.

can be observed. On the one hand, at the same normal stress, the shear strength of the RAP specimen with geogrid is greater than that without geogrid under a given test temperature. For example, when the normal stress is 50 kPa and the test temperature of 35°C, the shear strength of the RAP specimen without geogrid is 60.9 kPa, and it increases up to 77.1 after adding geogrid at the interface, with an increment of 16.2 kPa by 26.6%. This is because the presence of geogrid causes friction and interlock resistance between the geogrid and RAP, which enhances the shear strength [23]. On the other hand, the shear strength of RAP samples at lower test temperatures is higher than that at a higher temperature. For example, as the test temperature is 0°C, the values of shear strength of the RAP specimen with geogrid under 50, 75, and 100 kPa are 94.2, 117.3, and 140.6 kPa, respectively. In contrast, as the test temperature increases to 35°C, the corresponding shear strengths decrease to 77.1, 94.6, and 120.8 kPa, with an average decrease of about 17.2%. This indicates that the increase in test temperature exhibits an adverse effect on the development of shear strength. The possible reason is that the asphalt binder softens at high temperatures, resulting in a reduction in the shear strength of RAP-geogrid.

Since the linear relations between τ_f and σ obtained for pure RAP samples during the direct shear test, the Coulomb equation can be used to determine the shear strength parameters of RAP, as shown in Equation (1).

$$\tau_f = c + \sigma \tan \varphi, \tag{1}$$

where τ_f is the shear strength of the RAP sample, σ is the applied normal stress, and φ (internal friction angle) and c (cohesion) are the strength parameters.

For RAP samples with geogrid fixed at the interface, the Coulomb equation can also be used to determine the interface shear strength parameters of RAP-geogrid, as shown in Equation (2).

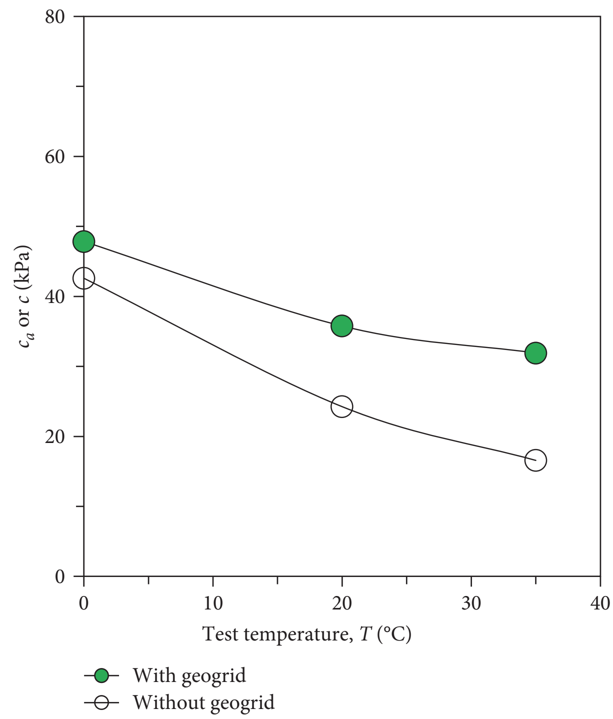

Figure 9: Variation of cohesion c or c_a with test temperature T for RAP specimens with or without geogrid.

$$\tau_f' = c_a + \sigma \tan \delta, \tag{2}$$

where τ_f' is the shear strength of the RAP sample with geogrid, σ is the applied normal stress, and δ (interface friction angle) and c_a (apparent adhesion intercept) are the strength parameters.

Figure 9 shows the change of c_a or c obtained from Equation (2) or Equation (1) as a function of test temperature T for RAP specimens with or without geogrid. It can be seen that both c_a or c shows a decreasing trend with the increase of the test temperature and tends to be stable as the temperature continues to increase. For example, when the test temperature increases from 0 to 20°C, the apparent adhesion intercept c_a of the RAP-geogrid decreases from 47.8 to 35.8 kPa by 25.1%. While the test temperature increases from 20 to 35°C, The value of c_a of the RAP-geogrid reduces from 35.8 to 31.9 kPa by 10.9%. This is because the increase in test temperature leads to the softening of asphalt binder and reduces the bond strength of asphalt coating at the interface of enhanced RAP. Moreover, the variation curve of apparent adhesion intercept c_a of RAP-geogrid versus temperature lies above the curve of cohesion c versus temperature of pure RAP specimen. In detail, as the test temperatures are 0, 20, and 35°C, the values of c_a are 42.6, 24.3, and 16.6 kPa, compared to the higher values of c with 47.8, 35.8, and 31.9 kPa, respectively. This is because of the interlock resistance between the RAP particles and geogrid, which increases the cohesion on the interface.

For a better description, the difference $\Delta c = (c_a - c)$ between apparent adhesion intercept c_a and the cohesion c

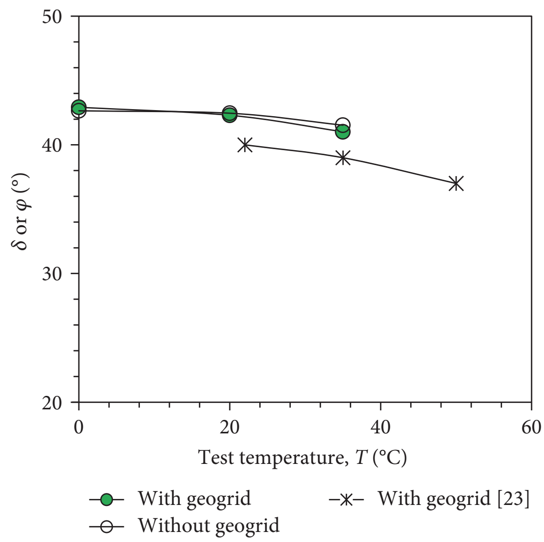

FIGURE 10: Variation of δ or φ with test temperature T for RAP specimens with or without geogrid.

TABLE 3: Comparison of interface shear strength parameters for various interface materials.

Geosynthetics—soil	Apparent adhesion intercept c_a (kPa)	Interface friction angle δ (°)	Soil or RAP cohesion c (kPa)	Soil or RAP internal friction angle φ (°)	Reference
Biaxial geogrid-RAP	47.8	42.9	42.6	42.6	This study (0°C)
Biaxial geogrid-RAP	35.8	42.3	24.3	42.5	This study (20°C)
Biaxial geogrid-RAP	31.9	41.0	16.6	41.5	This study (35°C)
Biaxial geogrid-RAP	39	37	25	39	Soleimanbeigi et al. [23]
Woven geotextile-RAP	20	22	25	39	Soleimanbeigi et al. [23]
Nonwoven geotextile-RAP	25	20	25	39	Soleimanbeigi et al. [23]
Uniaxial geogrid-RAP	26	29	25	39	Soleimanbeigi et al. [23]
Biaxial geogrid-gravel	6.2	45.9	–	–	Liu et al. [32]
Uniaxial geogrid-sand	27.7	37.8	21.0	27.3	Zhou et al. [33]
Uniaxial geogrid-gravel sand	23.4	28	3.1	30	Xu [34]
Geotextile-sand	–	37.3	–	–	[35]
Geotextile-sand	–	40.96	–	–	Sayeed et al. [36]

Note: Part of the data from Soleimanbeigi et al. [23] was at compaction temperature of 50°C and test temperature of 22°C.

for the RAP specimen at a given temperature can be obtained. It can be found that Δc gradually increases with increasing test temperature from 0 to 35°C. In detail, the value of Δc increases from 5.2 kPa at 0°C to 15.3 kPa at 35°C. Since the test temperatures of 0 and 35°C are, respectively, representative of the cold and hot seasons, the RAP-geogrid at such temperatures will behave with different properties. When simulating the representative temperature in the cold season (0°C), the RAP sample can maintain enough integrity because 0°C is the water's freezing point, regardless of whether it is reinforced with geogrid, leading to a small Δc. In contrast, as the representative temperature in the hot season (35°C), the advantages of geogrid are fully reflected. Although the asphalt binder absorbs heat and softens, resulting in a reduction in viscosity, the geogrid inside the reinforced RAP sample can still play a good role in embedding, forming a certain interlock resistance at RAP-geogrid interface, resulting in an increase of Δc.

Figure 10 shows the change of interface friction angle δ or internal friction angle φ obtained from Equation (2) or Equation (1) as a function of test temperature T for RAP specimens with or without geogrid. It can be seen that both δ and φ slightly decrease with the increase in test temperature. For comparison, the large-scale direct shear test result for RAP with biaxial geogrid was collected from Soleimanbeigi et al. [23] were collected and plotted in Figure 10. A similar slight decrease in interface friction angle with the test temperature can be seen. The possible reason is that the increase in temperature will slightly reduce the interface friction between RAP and geogrid. For example, when the temperature rises from 0 to 35°C, the internal friction angle of pure RAP specimen decreases from 42.6° to 41.5° by 2.6%, while the interface friction angle of RAP—geogrid decreased from 42.9° to 41.0° by 4.4%. The main reason is that the increase in temperature will weaken the friction and interlock resistance at the interface of the RAP-geogrid.

Noted that the interface shear strength parameters, i.e., apparent adhesion intercept c_a and interface friction angle δ are two key parameters for the design of reinforced RAP material as backfills, which can be used as alternative backfill materials to replace natural aggregates such as gravel and sand for geosynthetically reinforced mechanically stabilized earth (MSE) walls. Therefore, to verify the feasibility of RAP-geogrid, the shear strength parameters were compared with the strength parameters of sand, gravel, and geosynthetics interfaces used in traditional geotechnical engineering applications, as shown in Table 3. Compared with RAP-geosynthetics at a compaction temperature of 50°C and test temperature of 22°C by Soleimanbeigi et al. [23], this study shows similar results of RAP-geogrid at the same compaction temperature and test temperature of 20°C. This study further evaluates the effect of test temperatures on the interface strength parameters. For RAP-geogrid, the value of apparent adhesion intercept ranges from 31.9 to 47.8 kPa, which is higher than that for sand and gravel with geosynthetics. The interface friction angle ranges from 41.0° to 42.9°, which is close to that for sand and gravel with geosynthetics. For pure RAP, the value of cohesion ranges from 16.6 to 42.6 kPa, and the internal friction angle ranges from 41.5° to 42.6°, both of which are higher than that for sand and gravel, as shown in Table 3. Therefore, in terms of strength, the RAP can be well used as alternative backfill materials in lieu of natural aggregates such as gravel and sand in geotechnical applications.

4. Conclusions

In this study, a series of direct shear tests were conducted on compacted RAP samples and RAP-geogrid at different temperatures to investigate the influence of temperature on interface behaviors between compacted RAP and geogrid. The main conclusions are summarized as follows:

(1) Shear stress versus shear displacement curves of RAP specimens with or without geogrid show strain-softening characteristics. Under the same normal stress, the curve of the reinforced RAP sample with a high temperature is always below that with a low temperature, indicating that the test temperature has an adverse effect on the strength of the reinforced RAP sample.

(2) The shear strength consistently increases linearly with the increase of applied normal stress for all RAP samples. At the same normal stress, the shear strength of the RAP specimen with geogrid is greater than pure RAP under a given test temperature. The shear strength of RAP samples at lower test temperatures is higher than that at higher temperatures.

(3) Both apparent adhesion intercept and cohesion show a decreasing trend with the increase of the test temperature and tend to be stable as the temperature continues to increase. Moreover, the variation curve of the apparent adhesion intercept of RAP-geogrid versus temperature lies above the curve of cohesion versus temperature of pure RAP specimen. Both interface friction angle and internal friction angle slightly decrease with the increase of test temperature.

(4) For RAP-geogrid, the value of the apparent adhesion intercept is higher than those for sand and gravel with geosynthetics. The interface friction angle is close to that of sand and gravel with geosynthetics. For pure RAP, the values of cohesion and the internal friction angle are higher than that for sand and gravel. RAP can be well used as alternative backfill materials in lieu of natural aggregates such as gravel and sand in geotechnical applications such as geosynthetically reinforced MSE walls.

Note that the findings obtained in the present study are based on one source of RAP with asphalt binder content of 4.2% in China. The general trends, however, are expected to be similar if other sources of RAP are used. Further study is needed to address the effect of temperature on creep behavior at the interface of compacted RAP and geogrid.

Data Availability

All raw data can be provided by the corresponding authors upon request.

Conflicts of Interest

The authors declare that they have no conflicts of interest.

Acknowledgments

This study was financially supported by the National Natural Science Foundation of China (grant no. 51978315), which is gratefully appreciated.

References

[1] J. A. Gambatese and S. Rajendran, "Sustainable roadway construction: energy consumption and material waste generation of roadways," in *Proceedings of the Construction Research Congress*, pp. 104–110, ASCE, San Diego, California, April 05, 2005.

[2] A. C. Carpenter, K. H. Gardner, J. Fopiano, C. H. Benson, and T. B. Edil, "Life cycle based risk assessment of recycled materials in roadway construction," *Waste Management*, vol. 27, no. 10, pp. 1458–1464, 2007.

[3] J. Yin, A. Soleimanbeigi, W. J. Likos, and T. B. Edil, "Effects of temperature on creep behavior of compacted recycled asphalt pavement," *Journal of Geotechnical and Geoenvironmental Engineering*, vol. 143, no. 4, Article ID 06016028, 2017.

[4] Y. Zhu, F. Zhang, and S. Jia, "Embodied energy and carbon emissions analysis of geosynthetic reinforced soil structures," *Journal of Cleaner Production*, vol. 370, Article ID 133510, 2022.

[5] J. Gao, J. Yang, D. Yu et al., "Reducing the variability of multi-source reclaimed asphalt pavement materials: a practice in China," *Construction and Building Materials*, vol. 278, no. 9, Article ID 122389, 2021.

[6] K. R. Hansen and A. Copeland, "Annual asphalt pavement industry survey on recycled materials and warm-mix asphalt usage: 2009-2013," in *National Asphalt Pavement Association*

Report, National Asphalt Pavement Association, Lanham, MD, 2014.
[7] R. Mariyappan, J. S. Palammal, and S. Balu, "Sustainable use of reclaimed asphalt pavement (RAP) in pavement applications—a review," *Environmental Science and Pollution Research*, vol. 30, no. 16, pp. 45587–45606, 2023.
[8] E. M. Rathje, A. F. Rauch, D. Trejo et al., "Evaluation of Crushed Concrete and Recycled Asphalt Pavement as Backfill for Mechanically Stabilized Earth Walls," Texas Department of Transportation, Austin, TX, USA, Rep. FHWA/TX-06/0-4177-3, 2006.
[9] A. Copeland, "Reclaimed asphalt pavement in asphalt mixtures: state of the practice," in *Federal Highway Administration Report*, U.S. Department of Transportation, 2011.
[10] T. B. Edil, J. A. Tinjum, and C. H. Benson, "Recycled unbound materials," Minnesota Department of Transportation, Rep. MN/RC 2012-35, 2012.
[11] S. Saride, D. Avirneni, and S. C. P. Javvadi, "Utilization of reclaimed asphalt pavements in indian low-wolume roads," *Journal of Materials in Civil Engineering*, vol. 28, no. 2, Article ID 04015107, 2015.
[12] E. Mousa, S. El-Badawy, and A. Azam, "Evaluation of reclaimed asphalt pavement as base/subbase material in Egypt," *Transportation Geotechnics*, vol. 26, Article ID 100414, 2021.
[13] S. Barmade, S. Patel, and A. Dhamaniya, "Performance evaluation of stabilized reclaimed asphalt pavement as base layer in flexible pavement," *Journal of Hazardous, Toxic, and Radioactive Waste*, vol. 26, no. 1, Article ID 04021051, 2022.
[14] S. K. Pradhan and G. Biswal, "Utilization of reclaimed asphalt pavement (RAP) as granular sub-base material in road construction," *Materials Today: Proceedings*, vol. 60, pp. 288–293, 2022.
[15] C. Viyanant, E. M. Rathje, and A. F. Rauch, "Creep of compacted recycled asphalt pavement," *Canadian Geotechnical Journal*, vol. 44, no. 6, pp. 687–697, 2007.
[16] A. Soleimanbeigi, T. B. Edil, and C. H. Benson, "Effect of temperature on geotechnical properties of recycled asphalt shingle mixtures," *Journal of Geotechnical and Geoenvironmental Engineering*, vol. 141, no. 2, Article ID 04014097, 2015.
[17] J. K. Mitchell and K. Soga, *Fundamentals of Soil Behavior*, John Wiley & Sons, Inc, New York, 3rd edition, 2005.
[18] J. H. Yin, "Review of elastic visco-plastic modeling of the time-dependent stress-strain behavior of soils and its extensions and applications," in *Constitutive Modeling of Geomaterials*, Q. Yang, J. M. Zhang, H. Zheng, and Y. Yao, Eds., Springer Series in Geomechanics and Geoengineering, Springer, Berlin, Heidelberg, 2013.
[19] X. L. Lai, S. M. Wang, W. M. Ye, and Y. J. Cui, "Experimental investigation on the creep behavior of an unsaturated clay," *Canadian Geotechnical Journal*, vol. 51, no. 6, pp. 621–628, 2014.
[20] N. Sivasithamparam, M. Karstunen, and P. Bonnier, "Modelling creep behaviour of anisotropic soft soils," *Computers and Geotechnics*, vol. 69, pp. 46–57, 2015.
[21] F. L. Roberts, P. S. Kandhal, E. R. Brown, D. Y. Lee, and T. W. Kennedy, *Hot Mix Asphalt Materials, Mixture Design, and Construction*, National Asphalt Paving Association Education Foundation, Lanham, MD, 1996.
[22] J. K. Thakur, J. Han, and R. L. Parsons, "Creep behavior of geocell-reinforced recycled asphalt pavement bases," *Journal of Materials in Civil Engineering*, vol. 25, no. 10, pp. 1533–1542, 2013.
[23] A. Soleimanbeigi, A. Ozocak, B. Li et al., "Mechanical and hydraulic compatibility of RAP with geosynthetics used in MSE walls," *Geosynthetics International*, vol. 29, no. 1, pp. 1–37, 2021.
[24] ASTM, "Standard test method for particle-size analysis of soils," ASTM International, West Conshohocken, PA, 2007, D422-63(2007)e2. https://www.astm.org/.
[25] RMRC, "User guidelines for by-products and secondary use materials in pavement construction," 2014, May 1 2014. http://rmrc.wisc.edu/ug-mat-reclaimed-asphalt-pavement/.
[26] ASTM, "Standard test methods for specific gravity of soil solids by water pycnometer," ASTM International, West Conshohocken, PA, 2014, D854-14. https://www.astm.org/.
[27] ASTM, "Standard test methods for laboratory compaction characteristics of soil using standard effort (12,400 ft lbf/ft^3 (600 kN m/m^3))," ASTM International, West Conshohocken, PA, 2012, D698-12e2. https://www.astm.org/.
[28] J. Yin, X. G. Wang, M. M. Hu, and Y. Tang, "Direct shear creep tests on recycled asphalt pavement material with consideration of compaction temperature effect," *Journal of Jiangsu University (Natural Science Edition)*, vol. 41, no. 4, pp. 478–483, (in Chinese), 2020.
[29] ASTM, "Standard test method for direct shear test of soils under consolidated drained conditions," ASTM International, West Conshohocken, PA, 2011, D3080-11. https://www.astm.org/.
[30] C.-N. Liu, J. G. Zornberg, T.-C. Chen, Y.-H. Ho, and B.-H. Lin, "Behavior of geogrid-sand interface in direct shear mode," *Journal of Geotechnical and Geoenvironmental Engineering*, vol. 135, no. 12, pp. 1863–1871, 2009.
[31] N. Sudarsanan, R. Karpurapu, and V. Amrithalingam, "An investigation on the interface bond strength of geosynthetic-reinforced asphalt concrete using Leutner shear test," *Construction and Building Materials*, vol. 186, pp. 423–437, 2018.
[32] F. Y. Liu, Q. T. Zheng, J. Wang, and M. J. Ying, "Effects of particle shape on shear behaviors of interface between coarse-grained soil and geogrid," *Journal of Civil and Environmental Engineering*, vol. 43, no. 6, (in Chinese), Article ID 9, 2021.
[33] Z. G. Zhou, D. J. Kong, Z. F. Yang, X. Deng, and M. Gao, "Interfacial characteristics between high density polyethylence geogridds and different backfills," *Journal of China & Foreign Highway*, vol. 38, no. 3, pp. 296–300, (in Chinese), 2018.
[34] L. Y. Xu, *The Experimental Study on Geocell Reinforced Soil Retaining Wall*, Shijiazhuang Tiedao University. (in Chinese), 2019.
[35] M. Ghazavi and D. Ghaffari, "Experimental investigation of time-dependent effect on shear strength parameters of sand-geotextile interface," *Transactions of Civil Engineering*, vol. 37, no. 1, pp. 97–109, 2013.
[36] M. M. A. Sayeed, B. J. Ramaiah, and A. Rawal, "Interface shear characteristics of jute/polypropylene hybrid nonwoven geotextiles and sand using large size direct shear test," *Geotextiles and Geomembranes*, vol. 42, no. 1, pp. 63–68, 2014.